

Monomethoxy-4-aminoazobenzenes: a computational study

Krishna L. Bhat ^a, Harold S. Freeman ^b, Janardhan Velga ^c, Les Sztandera ^a,
Mendel Trachtman ^a, Charles W. Bock ^{a,*}

^aChemistry Department, School of Science and Health, Philadelphia University, School House Lane and Henry Avenue,
Philadelphia, PA 19144, USA

^bCollege of Textiles, North Carolina State University, Raleigh, NC 27695, USA

^cSchool of Textiles and Materials Technology, Philadelphia University, Philadelphia, PA 19144, USA

Received 21 March 2000; accepted 18 May 2000

Abstract

The structural and electronic properties of the positional isomers of monomethoxy-4-aminoazobenzene (*n*-OMe-AAB) have been investigated using density functional theory with a basis set that includes polarization functions on all the atoms. These azo dyes are of interest because their carcinogenic activities depend dramatically on the position (*n*) of the methoxy group, e.g. 3-OMe-AAB is a potent hepatocarcinogen in the rat, whereas 2-OMe-AAB is a non-carcinogen. While it is generally believed that the various isomers of OMe-AAB require metabolic activation via *N*-hydroxylation prior to reaction with cellular macromolecules, we have shown that there are structural and electronic features present in these isomers that correlate with their carcinogenic behavior. © 2000 Published by Elsevier Science Ltd.

Keywords: Azo dyes; Carcinogen; Density functional theory

1. Introduction

3-Methoxy-4-aminoazobenzene (3-OMe-AAB) is a potent hepatocarcinogen in the rat [1]. This azo dye requires metabolic activation to *N*-hydroxy-3-methoxy-4-aminoazobenzene (*N*-OH-3-OMe-AAB) prior to reaction with cellular macromolecules [2]. This conclusion is in accord with the observation that 3-OMe-AAB is mutagenic on the *Salmonella* mammalian mutagenicity assay (Ames test) only after activation with S-9, the 9000 g supernatant

fraction of liver homogenate, whereas *N*-OH-3-OMe-AAB is strongly mutagenic without S-9 activation [3,4]. Interestingly, changing the position of the methoxy group on the phenyl rings dramatically influences the carcinogenic behavior of the resulting compound [5]. For example, 2-OMe-AAB is noncarcinogenic in rats whereas 4'-OMe-AAB is carcinogenic, but to a lesser degree than 3-OMe-AAB. This carcinogenic potency of 2- and 4'-OMe-AAB correlates well with their mutagenic activity in the Ames' *Salmonella* test, where neither 2-OMe-AAB nor its *N*-hydroxy derivative, *N*-OH-2-OMe-AAB, is mutagenic even after treatment with S-9; 4'-OMe-AAB is very slightly mutagenic in TA98 and *N*-OH-4'-OMe-

* Corresponding author. Tel.: +1-215-951-2876; fax: +1-215-951-6812.

E-mail address: chuck@larry.texsci.edu (C.W. Bock).

AAB is clearly mutagenic without S-9 treatment [6]. Unfortunately, the carcinogenic/mutagenic activities of the remaining monomethoxy derivatives of 4-aminoazobenzene or their *N*-hydroxy analogs have not been reported (it is known that *N,N*-dimethyl-3-OMe-AAB is carcinogenic; see [7]). For comparison, we note that the parent compound, 4-aminoazobenzene is only weakly carcinogenic in rats, nonmutagenic in TA98 with or without S-9 activation and mutagenic in TA100 only in the presence of S-9 [6].

Although it is not entirely clear why there is a significant difference in the carcinogenic behavior of 2- and 3-OMe-AAB, Kojima et al. [1] have determined that *N*-OH-3-OMe-AAB has a significantly greater effect than *N*-OH-2-OMe-AAB on DNA synthesis in vivo. This suggests that the observed differences in the carcinogenic activity of 2-OMe-AAB and 3-OMe-AAB may be linked to the differences in the inhibitory effects of their *N*-hydroxy derivatives on DNA replication. Hashimoto et al. [8] have established that cytochrome P-450 enzymes efficiently catalyze the mutagenic activation of 3-OMe-AAB and, in contrast to other carcinogenic aromatic amines, the activation is mediated by phenobarbital-P-450 rather than by 3-methyl-cholanthrene-P-450.

Despite significant interest in the carcinogenic behavior of the various positional isomers of OMe-AAB, relatively little is known about their structural or electronic properties. No experimental results from X-ray or electron-diffraction studies have been reported for any of the OMe-AAB isomers. [Only a few experimental structures of azo dyes have been reported: *O*-aminoazotoluene (X-ray) [9]; Disperse Red 167 (X-ray) [10]; C.I. Disperse Yellow 86 (X-ray) [11]]. Furthermore, no high-level computational results that compare the various OMe-AAB isomers using either molecular orbital or density functional theory have been published. It is important to note that substitutions at the 2- and 6-positions or at the 3- and 5-positions in 4-aminoazobenzene are not equivalent (see Fig. 1). However, it is not evident that distinctions of this type were considered in the carcinogenic/mutagenic studies involving 2- and 3-OMe-AAB [1–5]. Thus, it is probably more appropriate to describe these studies as involving

methoxy-substitution at the *meta* and *ortho* positions, respectively. The purpose of the present paper is to describe the results of an extensive computational study using density functional theory (DFT) to establish the conformational preferences and relative energies of the positional isomers of OMe-AAB. Our goal is to identify any electronic and/or structural features that may exist among these positional isomers that can be correlated with their diverse carcinogenic behaviors and lead to a better understanding of the underlying molecular mechanism(s) involved.

2. Computational methods

Density functional calculations were performed at the BP/DN** computational level with SPARTAN v5.0 on Silicon Graphics computers [12]. This level uses the non-local Becke–Perdew (BP) 86 functional and employs the numerically defined DN** basis set which includes polarization functions on all the atoms [13,14]. Complete optimizations for a variety of conformers of each OMe-AAB derivative were carried out; no symmetry constraints were employed in order to minimize the likelihood of optimizing to a transition state. In a few cases frequency analyses were performed to ensure that the optimized structures were local minima on the potential energy surfaces (PESs). The graphics utilities of SPARTAN were used to examine the electron densities, electrostatic potentials and various Kohn–Sham orbitals for each conformer [12]. Mulliken and electrostatic charges were also calculated. For comparison, we performed a few optimizations at the B3LYP/6-31 + G* computational level [15] using the GAUSSIAN 98 series of programs [16].

3. Results and discussion

Since no experimental structural data are available even for the parent compounds azobenzene (AB) and 4-aminoazobenzene (AAB), we first optimized these molecules at the BP/DN** computational level. The initial structures of both AB and AAB were taken as nearly *trans* about the azo

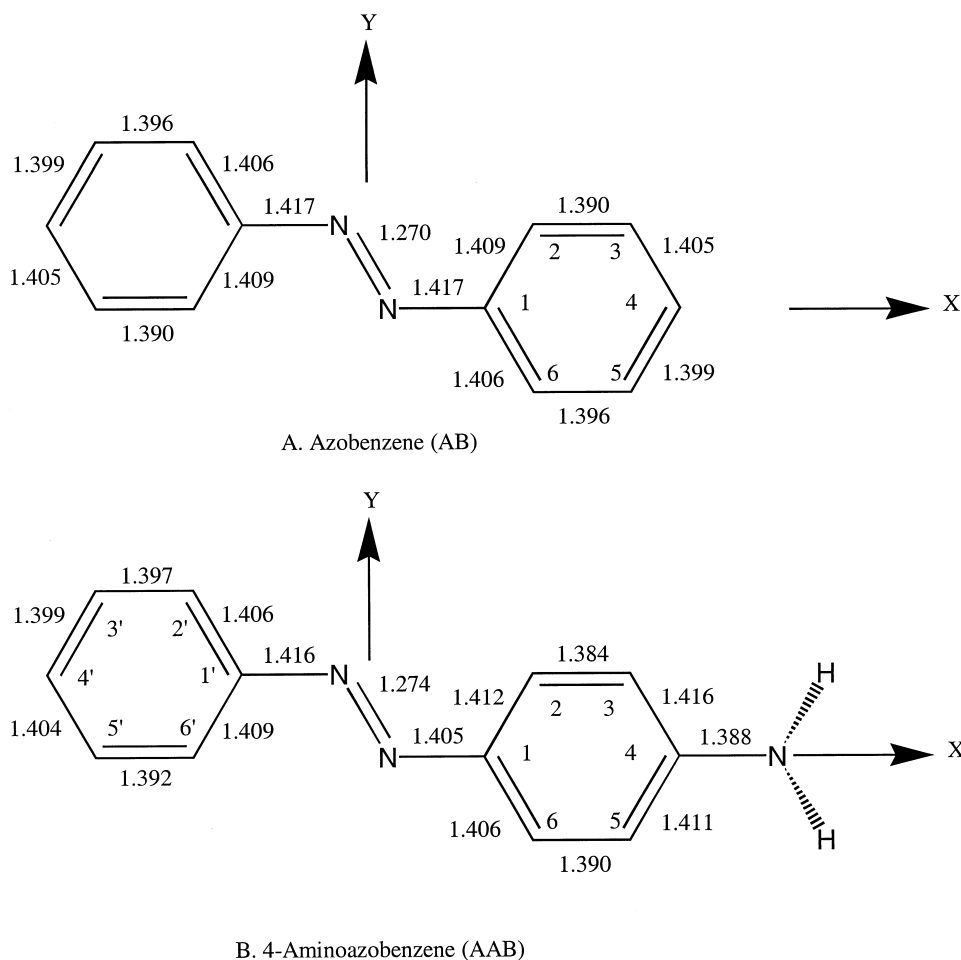


Fig. 1. The structures, coordinate system and numbering conventions for **A.** Azobenzene (AB) and **B.** 4-Aminoazobenzene (AAB). The bond lengths (Å) shown were calculated at the BP/DN**//BP/DN** computational level.

linkage¹ and, in the case of AAB, the amino group was taken as pyramidal with both hydrogen atoms on the same side of the ring.² The optimized structure of AB is found to be planar and a

¹ A second conformer of AB, with the phenyl rings twisted some 80°, was found to be 2.3 kcal/mol higher in energy at the BP/DN** computational level.

² We also optimized a conformer of AAB in which the hydrogen atoms bonded to the amine nitrogen atom are on opposite sides of the ring but otherwise the structure is planar. This conformer is 8.0 kcal/mol higher in energy than the form shown in Fig. 1. The optimized structure of a completely planar form of AAB is a transition state that is only 0.15 kcal/mol higher in energy than the lowest energy form shown in Fig. 1.

frequency analysis confirms that this is a local minimum on the PES. As can be seen in Fig. 1, the azo linkage in AB significantly distorts the carbon-carbon bond lengths in the phenyl rings compared to their values in benzene, where the carbon-carbon bond distances are 1.403 Å at this computational level. The length of the N=N bond in AB, 1.270 Å, suggests considerable electron delocalization; the calculated N=N bond lengths in CH₃-N=N-CH₃ and CH₃-N=N-C₆H₅ are shorter, 1.250 Å and 1.258 Å, respectively. Optimizations at the B3LYP/6-31+G* level show a similar trend, e.g. the N=N bond lengths in CH₃-N=N-CH₃ and AB are 1.241 and 1.258 Å,

respectively. In the optimized structure of AAB, the two phenyl rings are practically planar and nearly coplanar with each other. A frequency analysis confirms that this is a local minimum on the PES. To a large extent, the calculated structural parameters of AAB indicate that the amino group at the 4-position reinforces the geometrical changes already induced by the azo linkage. This is a consequence of electron delocalization using the lone pair of electrons from the amino nitrogen atom to give the C₄–N bond partial double bond character, which results in predictable adjustments of the bond lengths in the remainder of the molecule. For comparison, we note that the calculated lengths of the C–N bonds in CH₃–NH₂ and C₆H₅–NH₂ are 1.478 and 1.408 Å, respectively, considerably longer than that found in AAB, 1.388 Å.³ Nevertheless, the structure of the amino group in AAB remains pyramidal — the sum of the three bond angles is 346.7° at this computational level, compared to 318.4° and 325.6° for NH₃ and NH₂–CH₃, respectively.

It is of interest to compare a few of the Kohn–Sham molecular orbitals of AB and AAB. The highest occupied molecular orbital (HOMO) in AB is a lone-pair orbital localized primarily in the vicinity of the azo linkage, which is 14.4 kcal/mol above the next highest occupied orbital (HOMO{–1}), a delocalized *pi*-bonding orbital. The lowest unoccupied molecular orbital (LUMO) in AB is a *pi*-antibonding orbital, some 46.7 kcal/mol above the HOMO. In AAB the HOMO also involves the azo bond lone-pair electrons (see Fig. 2). It is nearly identical in shape to the HOMO found in AB, but it is 7.4 kcal/mol higher in energy. The HOMO{–1} in AAB involves the lone pair of electrons on the amino nitrogen atom (see Fig. 2), but otherwise it is similar in shape to the HOMO{–1} (*pi*-bonding orbital) in AB. However, this HOMO{–1} is 18.6 kcal/mol above its counterpart in AB, reducing the energy gap between the two highest occupied orbital in AAB to only 3.2 kcal/mol. The LUMO in AAB is similar in shape to the *pi*-antibonding LUMO in AB except that it includes a contribution from the

amine nitrogen atom (see Fig. 2). The energy gap between the HOMO and LUMO is 47.5 kcal/mol.

Two general types of conformers were considered for each of the positional isomers of monomethoxy AAB: one in which the O–Me bond is essentially in the nominal plane of the phenyl ring to which it is bonded and one in which the O–Me bond is nearly perpendicular to this ring. For all nine isomers, the conformers in which the O–Me bond lies essentially in the ring plane were found to be *lower* in energy at the BP/DN**//BP/DN** computational level; frequency analysis on this form of the 2-OMe, 3-OMe and 4'-OMe isomers confirm that these structures are local minima on their respective PESs. The energies for the conformers with the O–Me bond in the plane are listed in Table 1 along with those for AB and AAB. Selected geometrical parameters and properties for the various OMe-AAB isomers calculated at the BP/DN** level are listed in Tables 2 and 3. Since several orientations are possible for the methyl group, their positions for the lowest energy conformers at the BP/DN** level are shown in Fig. 3. It should be noted that energy differences between some of the conformers of these monomethoxy isomers were quite small. For example, rotating 180° about the C_o–O bond in 4'-OMe-AAB and reoptimizing yields a structure only 0.3 kcal/mol higher in energy, whereas a

Table 1

Total molecular energies (a.u.) and relative energies (kcal/mol) for *n*-methoxy-4-aminoazobenzenes calculated at the BP/DN**//BP/DN** computational level

<i>n</i>	Total molecular energies (a.u.) (BP/DN **//BP/DN**)	Relative energies
2	–742.931442	+ 6.7
3	–742.942450	0.0
5	–742.941042	+ 0.9
6	–742.936054	+ 4.0
2'	–742.935475	+ 4.4
3'	–742.940108	+ 1.5
4'	–742.940449	+ 1.3
5'	–742.941441	+ 0.6
6'	–742.930842	+ 7.3
AAB	–628.365269 ^a	–
AB	–572.974339 ^b	–

^a B3LYP/6-31 + G**//B3LYP/6-31 + G* = –628.144576 a.u.

^b B3LYP/6-31 + G**//B3LYP/6-31 + G* = –572.784293 a.u.

³ At the B3LYP/6-31 + G**//B3LYP/6-31 + G* computational level the C–NH₂ bond lengths in AAB and CH₃–NH₂ are 1.389 and 1.467 Å, respectively.

Table 2

Structural parameters [bond lengths (Å), bond angles (°)] for AB, AAB and *n*-OMe-AAB calculated at the BP/DN**//BP/DN** computational level

<i>n</i>	C ₁ –C ₂	C ₂ –C ₃	C ₃ –C ₄	C ₄ –C ₅	C ₅ –C ₆	C ₆ –C ₁	C ₄ –N	C ₁ –N	N=N
2	1.436	1.398	1.409	1.409	1.386	1.410	1.391	1.396	1.278
3	1.416	1.382	1.428	1.404	1.393	1.403	1.380	1.402	1.278
5	1.407	1.388	1.409	1.421	1.388	1.412	1.384	1.404	1.275
6	1.409	1.384	1.415	1.408	1.400	1.427	1.390	1.396	1.277
2'	1.411	1.384	1.415	1.410	1.392	1.407	1.392	1.406	1.277
3'	1.411	1.383	1.416	1.411	1.390	1.408	1.385	1.405	1.274
4'	1.412	1.385	1.415	1.410	1.390	1.407	1.390	1.404	1.276
5'	1.411	1.384	1.416	1.410	1.389	1.408	1.388	1.401	1.274
6'	1.412	1.383	1.414	1.410	1.392	1.406	1.392	1.412	1.277
AAB^b	1.412	1.384	1.416	1.411	1.390	1.406	1.388	1.405	1.274
	(1.410)	(1.385)	(1.414)	(1.408)	(1.390)	(1.404)	(1.389)	(1.408)	(1.262)
AB	1.409	1.390	1.405	1.399	1.396	1.406	–	1.417	1.270

<i>n</i>	C _{1'} –N	C _{1'} –C _{2'}	C _{2'} –C _{3'}	C _{3'} –C _{4'}	C _{4'} –C _{5'}	C _{5'} –C _{6'}	C _{6'} –C _{1'}	C ₆ –O	O–CH ₃	Σ <i>N</i> _z ^a
2	1.414	1.406	1.395	1.399	1.404	1.392	1.408	1.356	1.430	344.5
3	1.413	1.405	1.396	1.399	1.404	1.392	1.409	1.378	1.433	348.9
5	1.417	1.406	1.396	1.398	1.403	1.392	1.410	1.380	1.431	346.8
6	1.416	1.406	1.397	1.399	1.404	1.392	1.410	1.362	1.430	346.0
2'	1.404	1.425	1.404	1.398	1.401	1.392	1.406	1.364	1.431	344.6
3'	1.416	1.408	1.398	1.406	1.398	1.395	1.405	1.374	1.433	349.2
4'	1.411	1.408	1.389	1.406	1.408	1.391	1.406	1.370	1.432	345.7
5'	1.415	1.402	1.399	1.393	1.411	1.394	1.411	1.373	1.432	347.2
6'	1.401	1.410	1.390	1.397	1.398	1.404	1.432	1.359	1.433	345.2
AAB^b	1.416	1.406	1.397	1.399	1.404	1.392	1.409	–	–	346.7
	(1.419)	(1.403)	(1.396)	(1.398)	(1.402)	(1.392)	(1.408)			(346.7)
AB	1.417	1.406	1.396	1.399	1.405	1.390	1.404	–	–	–

^a Sum of three bond angles at the amine nitrogen atom.

^b The values in parentheses are at the B3LYP/6-31+G**//B3LYP/6-31+G* level.

conformer with the methyl group nearly perpendicular to the ring is 3.8 kcal/mol higher in energy.

3.1. 3- and 5-OMe-AAB

As can be seen from Table 1, 3-OMe-AAB has the lowest total molecular energy among all the positional isomers at the BP/DN**//BP/DN** computational level. However, the other *ortho* derivative, 5-OMe-AAB, is less than 1 kcal/mol higher in energy. As expected, the presence of a methoxy group *ortho* to the amino group perturbs the pattern of carbon–carbon bond lengths in the phenyl rings compared to those in AAB. The most prominent changes occur at the point of attachment; e.g. in the case of 3-OMe-AAB, the length of the shorter bond (C₂–C₃) decreases while the length of the longer bond (C₃–C₄) increases (see

Table 2). As might be expected, the lengths of the bonds in the unsubstituted phenyl ring are not significantly altered by the presence of the methoxy group. In both 3- and 5-OMe-AAB, the C₄–N bond length is shorter than that found in AAB and the amino group is less pyramidal (see Table 2). This suggests a further delocalization of the lone-pair electron density on the amino nitrogen atom; the calculated Mulliken and electrostatic charges on this nitrogen are less negative than those found in AAB. The C₆–O bond lengths in the 3- and 5-isomers, 1.378 and 1.380 Å, respectively, are *longer* than those calculated for the other positional isomers (see Table 2). In order to examine the effect of the amino group on the length of the C₆–O bond, we replaced it with a hydrogen atom in 3-OMe-AAB and reoptimized the structure. In the resulting 3-OMe-AB

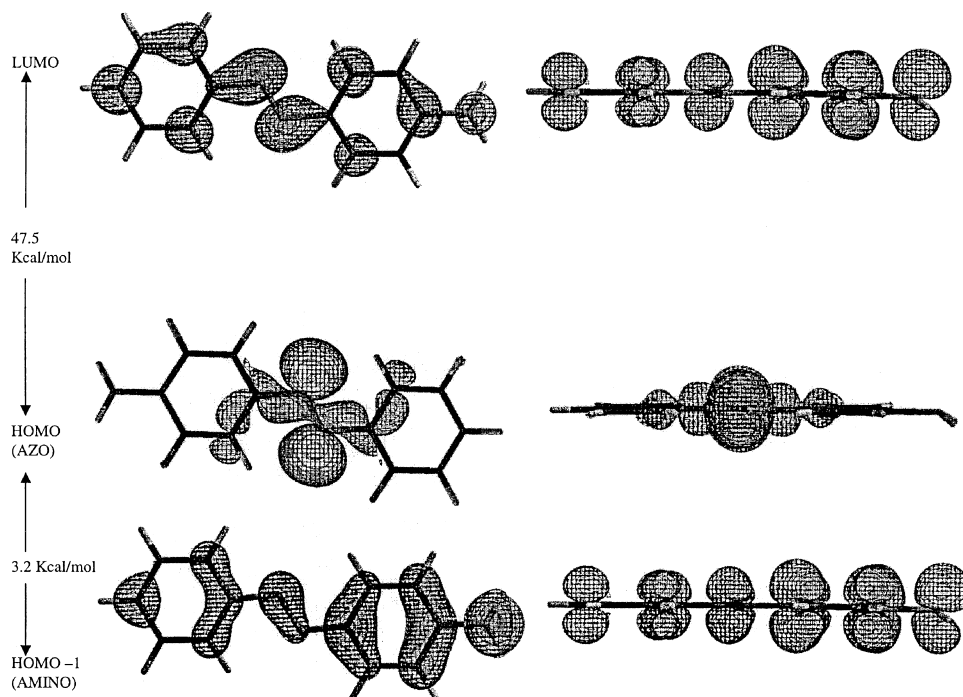


Fig. 2. The HOMO{−1}, HOMO and LUMO of 4-aminoazobenzene (AAB) calculated at the BP/DN**//BP/DN** computational level.

compound (as well as in $\text{MeO}-\text{C}_6\text{H}_5$) the $\text{C}_\text{o}-\text{O}$ bond length, 1.373 Å, is slightly shorter than that found in 3-OMe-AAB. Thus, the amino group at the 4-position tends to impede the delocalization of lone-pair density on the methoxy oxygen atom in 3-OMe-AAB.

The presence of a methoxy group *ortho* to the amino group in AAB has an interesting effect on the two highest occupied Kohn–Sham molecular orbitals. The orbital localized at the azo linkage in 3(5)-OMe-AAB is similar in shape and only 0.9 (1.5) kcal/mol higher in energy than the corresponding orbital in AAB; the in-plane lone pair on the methoxy oxygen is represented in this orbital, but to a rather small extent. The orbital involving the amino lone pair of electrons, which includes a significant contribution from the out-of-plane oxygen lone pair, is 5.3 (5.7) kcal/mol higher in energy than the corresponding orbital in AAB. This relatively large increase in energy makes it the HOMO in both 3- and 5-OMe-AAB. It is important to note that methoxy substitution at each of the positions on the phenyl rings increases the

energy of this orbital, but the increases for the 3- and 5-isomers are more than triple the smallest increase we observed, 1.7 kcal/mol for 5'-OMe-AAB. The relatively large increase in the energy of this orbital appears to be a result of electron overcrowding involving the proximate lone pairs on the methoxy oxygen and amino nitrogen atoms. The shape of the LUMO in 3(5)-OMe-AAB is quite similar to the LUMO in AAB, having relatively little contribution from the out-of-plane lone-pair orbital on the methoxy oxygen atom. Furthermore, the energy of these LUMO in both the 3- and 5-isomers is less than 2 kcal/mol above the LUMO in AAB. The energies separating the HOMO and LUMO in 3- and 5-OMe-AAB, 47.2 and 46.5 kcal/mol, are just slightly lower than that found in AAB.

3.2. 2- and 6-OMe-AAB

The positional isomers 2- and 6-OMe-AAB are 6.7 and 4.0 kcal/mol higher in energy than the lowest energy isomer, 3-OMe-AAB, at the BP/

Table 3

Selected properties for AB, AAB, and *n*-OMe-AAB calculated at the BP/DN**//BP/DN** computational level

<i>n</i>	HOMO{−1} (a.u.)	HOMO (a.u.)	LUMO (a.u.)	Log <i>P</i> ^d	Electrostatic charge on amino nitrogen atom	Dipole moment (D)
2	−0.186080 ^a	−0.171712 ^b	−0.101479	2.25	−0.72	4.85
3	−0.186278 ^b	−0.184263 ^a	−0.109082	2.13	−0.67	3.52
5	−0.185290 ^b	−0.183553 ^a	−0.109506	2.19	−0.67	3.54
6	−0.185048 ^a	−0.179274 ^b	−0.106652	2.26	−0.72	5.08
2'	−0.183749 ^a	−0.179501 ^b	−0.107565	2.29	−0.72	2.77
3'	−0.188844 ^a	−0.186038 ^b	−0.110120	2.24	−0.73	4.54
4'	−0.183084 ^c	−0.182205 ^c	−0.104728	2.34	−0.72	2.55
5'	−0.189970 ^a	−0.187243 ^b	−0.110805	2.53	−0.71	4.50
6'	−0.183052 ^a	−0.173803 ^b	−0.102735	2.30	−0.72	2.04
AAB	−0.192206 ^a	−0.187648 ^b	−0.111910	2.47	−0.72	3.61
AB	−0.222337 ^a	−0.199380 ^b	−0.126611	3.30	—	0.07

^a Orbital involves amino nitrogen lone pair.^b Orbital involves azo bond lone pairs.^c Orbital is mixed, see text.^d Log *P* is the logarithm of the octanol–water partition coefficient calculated using the Dixon–Hehre algorithm in Spartan 5.0. [12] This involves explicit evaluation of AM1_{oct} and AM1_{aq} solvation models. The Ghose–Crippen approach gives Log *P* = 3.54 for all the OMe-AAB isomers (Chase AK, Pritchett A, Crippen GM. J Comp Chem 1988;9:80).

DN**//BP/DN** computational level (see Table 1). The length of the C₄–N bond in both of these isomers is slightly longer than that found in AAB and the amino group is more pyramidal (see Table 2). The calculated Mulliken and electrostatic charges on the amino nitrogen atom in the 2- and 6-isomers are nearly the same as those in AAB. However, the C₆–O bond lengths in 2(6)-OMe-AAB, 1.356 Å (1.362 Å), are some 0.02 Å shorter than the corresponding bond lengths in 3(5)-OMe-AAB. This indicates further delocalization involving the oxygen out-of-plane lone pair, which gives the C₆–O bond additional double-bond character. The Mulliken charge on the oxygen atom in 2-OMe-AAB is not as negative as that found in 3-OMe-AAB. To examine the effect of the amino group on the length of the C₆–O bond in 2-OMe-AAB, we optimized the structure of the 2-OMe-AB. The length of the C₆–O bond increases, but only by about 0.002 Å; this change, however, is in a direction opposite to what we observed in going from 3-OMe-AAB to 3-OMe-AB. The shorter C₆–O bond in 2(6)-OMe-AAB results in an elongation of both carbon–carbon bonds in the ring at the point of methoxy attachment when compared to that in AAB (see

Table 2). Again, there are no significant changes in the carbon–carbon bond lengths in the unsubstituted phenyl ring compared to those in AAB.

The presence of a methoxy group *meta* to the amino group in AAB alters the two highest occupied Kohn–Sham orbitals differently than when the replacement occurs at an *ortho* position. In particular, the azo lone-pair orbital in 2(6)-OMe-AAB is 10.0 (5.3) kcal/mol higher in energy than the corresponding orbital in AAB, but only 0.9 (1.5) kcal/mol higher for substitution at the 3(5)-position. This orbital involves contributions from the azo nitrogen lone pairs and from the in-plane methoxy oxygen lone-pair; its relatively large increase in energy is clearly the result of adverse lone-pair interactions in the region. The particular geometrical arrangement of atoms in the vicinity of the *trans* azo linkage causes the electron overcrowding in this region to be more severe for methoxy substitution at the 2-position than at the 6-position. This leads to a greater increase in the energy of the azo lone pair orbital in 2-OMe-AAB and results in the largest energy gap between the two highest occupied orbitals we observed in this study, 9.0 kcal/mol. The orbital involved with the amino nitrogen lone pair in 2(6)-

OMe-AAB is similar in shape to the corresponding orbital in AAB, although it includes a contribution from the out-of-plane oxygen lone pair. Its energy is raised to a slightly lesser extent than it is when the methoxy group is at an *ortho* position. Thus, for 2(6)-OMe-AAB and AAB the orbital involving the azo lone pair is higher in energy than the orbital involving the amino nitrogen lone pair, whereas for 3(5)-OMe-AAB the order of these two orbitals is reversed. It is also interesting to note that the energy gap between the two highest occupied molecular orbitals in 2(6)-OMe-AAB, 9.0 (3.6) kcal/mol, is greater than that in AAB, 3.2 kcal/mol, and in 3(5)-OMe-AAB, 1.3 (1.1) kcal/mol. The LUMO in both the 2- and 6-isomers is similar in shape to that in AAB, but involves a significant contribution from the out-of-plane lone-pair orbital on the methoxy oxygen atom. The LUMO energies of 2- and 6-OMe-AAB are higher than those of 3- and 5-OMe-AAB,

whereas the separation in energy between the HOMO and LUMO are smaller, 44.1 and 45.6 kcal/mol, respectively.

3.3. 3'- and 5'-OMe-AAB

The positional isomers 3'(5')-OMe-AAB are only 1.5 (0.6) kcal/mol higher in energy than 3-OMe-AAB (see Table 1). Interestingly, methoxy substitution at the 3'- or 5'-position has very little effect on the carbon-carbon bond lengths in either of the phenyl rings when compared to those in AAB (see Table 2). The C₄-N bond length in 3'-OMe-AAB is slightly shorter than that found in AAB while that of 5'-OMe-AAB is nearly the same as in AAB. The small differences in the geometrical parameters and the lack of any severe lone-pair interactions in 3'(5')-OMe-AAB are consistent with the observation that the two highest occupied Kohn–Sham orbitals of AAB are

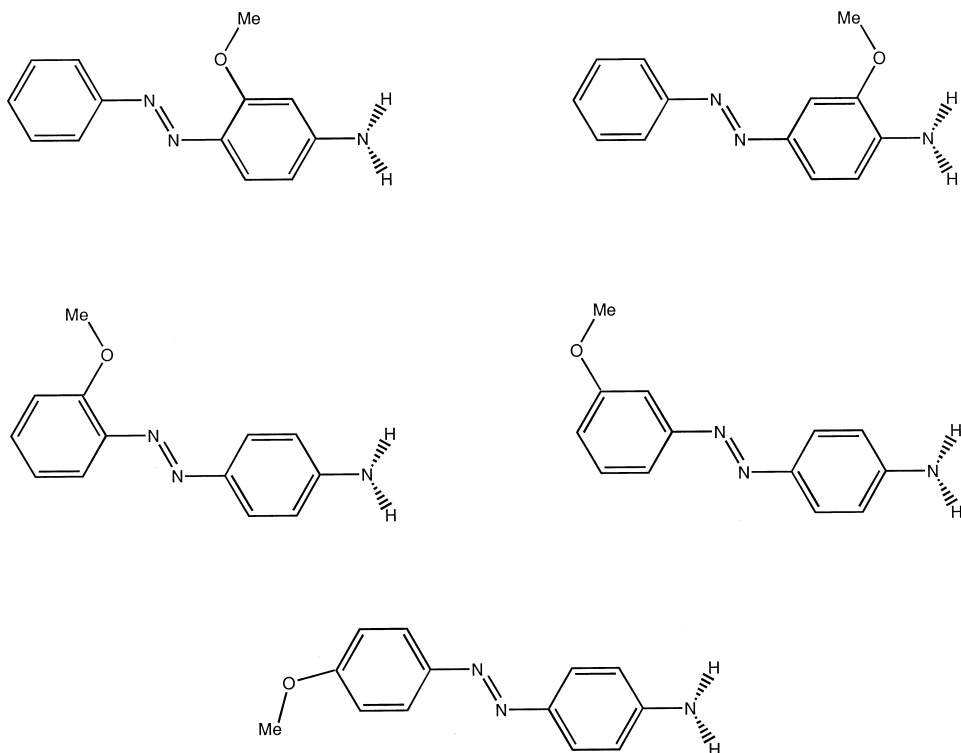


Fig. 3. The orientation of the methyl group for the positional isomers of monomethoxy-4-aminoazobenzene calculated at the BP/DN**//BP/DN** computational level. (The orientation of the methyl group in 6-OMe-AAB is analogous to that for 2-OMe-AAB, etc.)

closer in energy to those of 3'(5')-OMe-AAB than to those of the other positional isomers. The azo and amino nitrogen lone-pair orbitals are only 1.0 (0.3) and 2.4 (1.7) kcal/mol higher in energy than the corresponding orbitals in AAB, leading to a small energy gap of 1.8 (1.7) kcal/mol. The structure of the LUMOs are again similar in shape to that found in AAB, with relatively little contribution from the out-of-plane oxygen lone-pair orbital; the HOMO–LUMO energy gaps, 47.6 and 48.0 kcal/mol, are slightly greater than that found in AAB.

3.4. 2'- and 6'-OMe-AAB

The positional isomers 2'- and 6'-OMe-AAB are found to be 4.4 and 7.3 kcal/mol higher in energy than 3-OMe-AAB (see Table 1). As can be seen in Table 2, methoxy substitution at the 6'-position of AAB leads to greater changes in several of the geometrical parameters than those found with the other monomethoxy derivatives. The relatively short C_{6'}–O bond length, 1.359 Å, in 6'-OMe-AAB indicates significant electron donation from the out-of-plane lone pair on the methoxy oxygen. This short C_{6'}–O bond is compensated for by an elongation of both carbon–carbon bonds in the ring involving the C_{6'} atom, a shortening of the C_{1'}–N bond and a slight elongation of the N=N bond. Analogous changes in the bond lengths occur for substitution at the 2-position, but the presence of the amino group limits the magnitude of these changes somewhat, particularly at the azo linkage (see Table 2). The energies of the highest two Kohn–Sham molecular orbitals in AAB are both significantly increased by substitution at the 6'-position. The lone-pair orbital localized at the azo linkage also includes a contribution from the in-plane oxygen lone pairs and remains higher in energy than the orbital involving the amino nitrogen lone pair; the energy separation, 5.8 kcal/mol, is the second highest we observed for any of the monomethoxy derivatives. The structure of the LUMO is similar to that in AAB, but contains a contribution from the out-of-plane oxygen lone-pair, similar to that observed for the 2- and 6-isomers. The energy separations between the HOMO and LUMO are 45.1 and 44.6 kcal/mol, respectively.

3.5. 4'-OMe-AAB

The positional isomer 4'-OMe-AAB is only 1.3 kcal/mol higher in energy than 3-OMe-AAB (see Table 1). As can be seen in Table 2, the C_{4'}–O bond length, 1.370 Å, is intermediate between that found for the 3-, 3'-, 5- and 5'-isomers and that found for the 2-, 2'-, 6- and 6'-isomers. The pattern of carbon–carbon bond lengths in the phenyl ring to which the methoxy group is attached is generally enhanced above that already found in AAB. The structure of the two highest occupied Kohn–Sham molecular orbitals are radically different from those observed for the other positional isomers. They are nearly degenerate (only separated by 0.5 kcal/mol) and appear as a mixture of the orbitals involving the azo and amino nitrogen lone pairs that are found for the other positional isomers. For comparison, we optimized several other AAB derivatives with substitution at the 4'-position. Similar combination orbitals are obtained for the HOMO and HOMO{-1} of 4'-OH-AAB, but for 4'-F-AAB the HOMO is clearly an azo lone-pair type orbital, whereas for 4'-SMe-AAB the HOMO is an amine lone-pair type orbital. The structure of the LUMO in 4'-OMe-AAB is similar to that observed for AAB, but with a contribution from the out-of-plane lone-pair orbital on the oxygen atom; the energy gap between the HOMO and LUMO is 48.6 kcal/mol.

4. Concluding remarks

The methoxy-substituted azobenzene dyes 2-OMe-AAB, 4'-OMe-AAB and 3-OMe-AAB are noncarcinogenic, moderately carcinogenic and strongly carcinogenic, respectively [5]. The studies that established these results, however, have not made a clear distinction between methoxy substitution at the 2- and 6-positions or at the 3- and 5-positions. Results of *Salmonella* mutagenicity tests suggest that none of these molecules are mutagenic per se, but require activation prior to reaction with cellular macromolecules. Nevertheless, there appear to be some differences in the structures and electronic properties of the monomethoxy-AAB compounds that may provide a basis for understanding their diverse carcinogenic behavior.

Many of the structural features in the monomethoxy AAB derivatives are determined to a large extent by electron delocalization at the azo linkage, which establishes the pattern of carbon-carbon bond lengths in the phenyl rings of AB; this pattern is enhanced by electron delocalization at the amino nitrogen atom in AAB. The presence of a methoxy group, with its two lone pairs of electrons, provides yet another site where delocalization is an issue, but it also introduces the possibility of lone-pair interactions involving the azo and amino nitrogen lone pairs.

Comparing the structures of 3(5)-OMe-AAB with those of 2(6)-OMe-AAB suggests that there is competition to delocalize lone-pair electron density at the amino nitrogen and methoxy oxygen atoms. For the 3(5)-isomers, where the methoxy oxygen is in close proximity to the amino nitrogen, it is energetically favorable to delocalize at the (less-electronegative) amino nitrogen atom by further increasing the double bond character of the C₄–N bond; for these isomers the C₆–O bond is relatively long. For the 2(6)-isomers, where the methoxy oxygen is now in close proximity to the azo linkage, it becomes favorable to delocalize more at the methoxy oxygen atom by further increasing the double bond character of the C₆–O bond; for these isomers the C₄–N bond is relatively long.

The Kohn–Sham HOMO and HOMO{–1} of AAB involve the azo and amino lone pairs, respectively, and these orbitals are relatively close in energy. For most of the monomethoxy AAB derivatives, the two highest occupied orbitals are similar in shape to those found in AAB, but involve contributions from one of the two lone pairs on the methoxy oxygen atom. In these *n*-OMe-AAB compounds, the energies of the two highest occupied orbitals are sensitive to the position (*n*) of the methoxy group because there is the potential for its lone pairs to be forced into close proximity with those on the AAB backbone.

It is interesting to note that the HOMO of the strongest carcinogen, 3(5)-OMe-AAB, involves the amino nitrogen lone pair, whereas the HOMO of the noncarcinogen, 2(6)-OMe-AAB, involves the azo bond lone pairs. In the case of AAB itself, which is weakly carcinogenic, the HOMO also involves the azo bond lone pairs, but the separation

in energy between the two highest orbitals is *smaller* than that for 6-OMe-AAB and *substantially smaller* than that for 2-OMe-AAB. The carcinogenic potency of 4'-OMe-AAB is in between that of 2(6)-OMe-AAB and 3(5)-OMe-AAB and its HOMO is a mixed orbital that includes a contribution from the amino nitrogen lone pair.

The results of our investigation suggest that the carcinogenic activity of an OMe-AAB isomer is *increased* as the energy of the orbital involving the amino nitrogen lone pair is *raised* relative to that of the orbital involving the azo bond nitrogen lone pairs.⁴ This correlation can be further tested by noting that *N*-methyl-AAB and *N,N*-dimethyl-AAB compounds are usually *more* carcinogenic than the corresponding AAB compounds [6]. The HOMOs of both AAB and *N*-methyl-AAB are both localized at the azo linkage. However, the separation in energy between the HOMO and HOMO{–1} in *N*-methyl-AAB is only about 50% of the corresponding separation in AAB. On the other hand, the HOMOs of both 3-OMe-AAB and *N*-methyl-3-OMe-AAB involve the amino nitrogen lone pair, but for these compounds the energy gap between the two highest occupied orbitals is three times *greater* in the *N*-methyl compound. Furthermore, the HOMO and HOMO{–1} of *N,N*-dimethyl-AAB are of the mixed type we observed in 4'-OMe-AAB, where both orbitals involve the amino nitrogen lone pair. These results are consistent with an increase in the carcinogenic potency of a methoxy AAB derivative when the primary amine is monomethylated or dimethylated. It must be pointed out that a variety of effects can influence the carcinogenic activity of a particular compound [17–19]. For example, the HOMO of *N,N*-dimethyl-4'-OH-AAB involves the amino nitrogen lone pair and it is 2.7 kcal/mol *higher* in energy than the orbital involving the azo bond lone pairs. Based on our results for 2- and 3-OMe-AAB, this would suggest that *N,N*-dimethyl-4'-OH-AAB was a strong hepatocarcinogen in the rat, but this is not the case [20]. It is likely that the

⁴ The energies of the LUMOs do not seem to correlate well with the carcinogenic potency of the AAB compounds; e.g. the LUMO of the noncarcinogen 2-OMe-AAB is 4.4 kcal/mol above the LUMO of the strong carcinogen 3-OMe-AAB but 6.5 kcal/mol above the LUMO of the weak carcinogen AAB.

hydroxy group provides a site for the metabolic breakdown of this dye before it can act as a carcinogen [20]. In fact, studies have shown that *N,N*-dimethyl-4'-OH-AAB is formed from *N,N*-dimethyl-AAB during its metabolism by rat homogenates [21], and that demethylated hydroxyazo derivatives are present in the urine of rats fed the dye [22]. Additional calculations and further experimental carcinogenic/mutagenic studies on AAB derivatives will be required to establish the extent to which knowing the relative energies of the orbitals involving the azo bond and amino nitrogen lone pairs in these compounds can be used as a predictive tool of the carcinogenic behavior of azo dyes. These studies are currently in progress.

Acknowledgements

The authors would like to thank Brandon Francis for technical assistance. C.W.B., M.T. and L.S. would also like to acknowledge the National Textile Center (Grant No. I98-P01) for financial support of this research; Dr. Bhat would like to acknowledge the Lindback Foundation for financial support of this work.

References

- [1] Kojima M, Degawa M, Hashimoto Y, Tada M. *Biochem Biophys Res Commun* 1991;179:817.
- [2] Hashimoto Y, Degawa M, Watanabe HK, Tada M. *Gann* 1981;72:937.
- [3] Degawa M, Miyairi S, Hashimoto Y. *Gann* 1978;69:367.
- [4] Degawa M, Shoji Y, Masuko K, Hashimoto Y. *Cancer Lett* 1979;8:71.
- [5] Miller JA, Miller EC. *Cancer Res* 1961;21:1068.
- [6] Hashimoto Y, Watanabe HK, Degawa M. *Gann* 1981;72:921.
- [7] Stilborova M, Matrká M, Hradek J. *Biochem Pharmacol* 1980;29:2301.
- [8] Degawa M, Kojima M, Hashimoto Y. *Mutat Res* 1985;152:125.
- [9] Kurosaki S, Kashino S, Haisa M. *Acta Cryst* 1976;B32:3160.
- [10] Freeman HS, Posey Jr JC, Singh P. *Dyes and Pigment* 1992; 20:279.
- [11] Lye J, Hinks D, Freeman HS. Computational chemistry applied to synthetic dyes. In: Cisneros G, Cogordan JA, Castro M, Wang C, editors. *Computational chemistry and chemical engineering*. Singapore World Scientific Publ., 1997.
- [12] Spartan v.5.0, Wavefunction Inc., 18401 Von Karmen Avenue, Suite 370, Irvine, CA 92612, USA.
- [13] Perdew JP. *Phys Rev* 1986;B33:8822.
- [14] Perdew JP. *Phys Rev* 1987;B34:7046.
- [15] Gill PMW, Johnson BG, Pople JA, Frisch M. *J Chem Phys Lett* 1992;197:499.
- [16] Frisch MJ, Trucks GW, Schlegel HB, Scuseria GE, Robb MA, Cheeseman JR. et al. Pittsburgh, (PA) Gaussian, Inc. 1998.
- [17] Chung KT, Cerniglia CE. *Mutat Res* 1992;277:201.
- [18] Ashby J, Paton D, Lefevre PA, Styles JA, Rose FL. *Carcinogenesis* 1982;3:1277.
- [19] Cunningham AR, Klopman G, Rosenkranz HS. *Mutat Res* 1998;405:9.
- [20] Miller JA, Sapp RW, Miller EC. *Cancer Res* 1949;9:652.
- [21] Mueller GC, Miller JA. *J Biol Chem* 1948;176:535.
- [22] Miller JA, Miller EC. *Cancer Res* 1947;7:39.